*Progress In Electromagnetics Research, PIER 101, 1–16, 2010*

# METAL-BASED $1 \times 2$ AND $1 \times 4$ ASYMMETRIC PLASTIC OPTICAL FIBER COUPLERS FOR OPTICAL CODE GENERATING DEVICES

**A. A. Ehsan and S. Shaari**

Institute of Microengineering and Nanoelectronics
Universiti Kebangsaan Malaysia
Bangi, Selangor, Malaysia

**M. K. Abd Rahman**

Faculty of Applied Science
Universiti Teknologi MARA
Shah Alam, Malaysia

**Abstract**—An optical code generating device has been developed based on $1 \times 2$ and $1 \times 4$ asymmetric plastic optical fiber (POF) couplers. The code generating device provides a unique series of output power which are successively used as an optical code in a portable optical access-card system. The system is designed where the asymmetric POF coupler is embedded in an all passive portable unit. This device utilizes a tap-off ratio (TOFR) technique based on a simple variation of the tap width of an asymmetric Y-branch splitter design. A hollow-type waveguide structure is used where it eliminates the use of polymeric material for the waveguide core and allows simple fabrication and assembling of the device. The asymmetric POF coupler has been fabricated on metal-based materials using machining technique. The results for the simulated and fabricated $1 \times 2$ asymmetric couplers show the same linear characteristics between the TOFR and the tap width. The simulated devices shows a TOFR variation from 18.6% to 49.9% whereas the TOFR for the fabricated metal-based devices varies from 10.7% up to 47.7%, for a tap width of 500 µm to 1 mm. The $1 \times 4$ coupler designed using simple cascading of a Y-branch splitter with two $1 \times 2$ asymmetric couplers has been fabricated and shows similar characteristics as that of the designed $1 \times 4$ devices. The insertion loss for the $1 \times 2$ asymmetric coupler at the tap line varies from 9 dB to

Corresponding author: A. A. Ehsan (aaehsan@eng.ukm.my).

16 dB whereas for the bus line, the insertion loss is about $9 \pm 0.8$ dB. The insertion loss for the $1 \times 4$ asymmetric coupler at the output ports varies from 14 dB to 22 dB.

## 1. INTRODUCTION

The burst of global information technology has set off the need for transmission of enormous amount of data over short as well as very long distances. This demand for high capacity data transmission over both short and long hauls has become an increasingly everyday necessity. In addition to the conventional single mode optical fiber, a new type of optical fiber namely the Plastic Optical Fiber (POF) has been around for nearly 30 years. Due to its high attenuation and the lack of demand of specific commercial applications, POF had remained rather stagnated for years. However, since the invention of the graded-index plastic optical fibers by Professor Koike at Keio University (1990) and the development of the low attenuation perfluorinated fibers (1996), a lot of interests on POF have been received, which to give rise to a great deal of applications [1].

In addition to the data and optical communication applications, POF technology is also being used in automotive system, in-flight entertainment for airplane and optical interconnects for computer system. In sensor development, POF has established wide use in multimode intensity-based sensor applications [2]. These are some of the POF applications well known, however the used of POF technology for physical access to restricted facilities has not been ventured yet.

There are previous reports on the used of optical technology for security access system, however, these systems do not utilize planar optical waveguides or the concept of applying a unique series of optical power for code generation in an access-card system. They basically used fiber optics bundle where the codes are represented by the linear pattern of lighted and unlighted fibers, done by obscuring, breaking or omitting selected fiber in the bundle [3, 4]. The security access system developed by the NASA Research Center is one of a system that utilizes optical component for optical code generation. This system uses fiber Bragg gratings (FBG) as its code generating device [5]. Another system by Lawrence Livermore's Defense and Nuclear Technologies and Engineering Directorate have also developed a similar optical key component named *Light Lock Optical Security System* [6]. However, the major disadvantage of the system developed by NASA Research Center and Lawrence Livermore's Lab is the use of high cost single mode optical components and both the laser and power supply units have to be built into the portable key respectively.

In this paper, we report an optical code generating device to be implemented in a newly developed portable optical access-card system. The code generating device has been developed based on a $1 \times N$ asymmetric POF coupler. A $1 \times 2$ asymmetric POF coupler will be the fundamental component in this code generating device. The device design structure allows various ratios of optical output power to be generated which are then used as the optical codes. In addition to a simple $1 \times 2$ asymmetric coupler, a $1 \times 4$ asymmetric coupler has also been designed and fabricated. The $1 \times 2$ and $1 \times 4$ asymmetric couplers are designed and then modeled using non-sequential ray tracing tool. The device is constructed using metal-based material where the design structure is engraved onto the metal block using high speed CNC machine. The core region is based on a simple hollow structure which makes the device fabrication and assembling much simpler.

## 2. SYSTEM AND DEVICE DESIGN

The heart of the portable optical access-card system will be the asymmetric coupler device. This device can have $N$-number of output ports and one input port. An asymmetrical waveguide design is used to design the device which allows the input power to be split into any value from 0% to 100%.

Figure 1 is a block diagram showing how the output power of the code generating device are utilized for generating a unique optical code for the access-card system. In this figure, a generic $1 \times 4$ coupler is shown ($N = 4$, 4-digit code). The characters A, B, C and D represent generic terms for the codes. By a simple arrangement of the output power, a series of optical codes can be produced. Two examples of optical codes generated are shown in this figure. Each output port provides a unique output power which is achieved by a special design of the coupler. The value for the output power can be easily controlled by using the asymmetric coupler design.

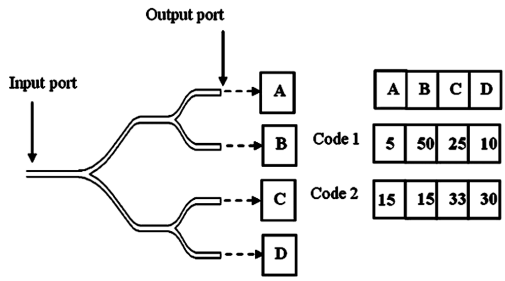


**Figure 1.** Code generating component: $1 \times 4$ coupler device.

We will assume the asymmetric coupler to be a $1 \times N$ coupler, which means $N$ number of output ports where $N$ is a positive integer, $N \geq 1$. Each of the output port may have different optical power values. The solution to the number of possible codes that can be generated, $K_N$ has been obtained using combinatory number theory and is shown as follows [7]:

$$K_N = \begin{pmatrix} M_{\max} + N \\ N \end{pmatrix} \tag{1}$$

where $N$ is the number of output ports of the waveguide coupler and $M_{max}$ is the maximum output power ratio of the waveguide which is taken as 100.

Theoretically, the power span for each of the output port can be taken from 0% and up to 100% of the input power. Hence, any output port can have its power to be as low as 0% or 100% of the input power. For the latter situation, this means only one detected output power which give 100% at only one output port.

The POF coupler is embedded in a portable unit without the need of any active components such as battery or laser diode. The optical light source or Light Emitting Diode (LED) will be positioned at the receiver section. The coupling of the LED and the POF coupler is done using a short 1 mm core size POF fiber (as part of the portable unit).

An important aspect of this asymmetric coupler is the size of waveguide core which has been chosen to allow us to couple the asymmetric coupler to a standard 1 mm core POF fiber. A hollow-type structure has been proposed where it eliminates the use of polymeric material for the waveguide core. This hollow structure allows simple fabrication and assembling of the optical code generating device. In order to account for any marginal errors due to low resolution of output power level, coupling loss between POF fibers and the waveguide, and POF fibers' bends and connectors losses, only the power detected at the receivers will be used as the actual optical code.

One main feature of the asymmetric coupler will be the tap-off ratio (TOFR) for an asymmetric Y-junction splitter device, which has been demonstrated by J. D. Love [8] where it allows simple optical power tap. In addition, a linear taper is included which enables the use of large core POF fiber to be coupled to the smaller size optical tap branch. Fig. 2 illustrates our simple $1 \times 2$ asymmetric coupler. This design is achieved by varying the width of the tap line. Using the concept structure in Fig. 2, we can generate several types of asymmetric coupler with any combinations of splitting ratio. There are a few distinct differences between the proposed asymmetric POF coupler and the asymmetric Y-junction splitter:

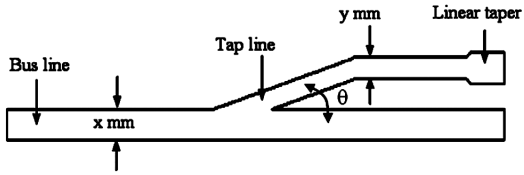


**Figure 2.** $1 \times 2$ asymmetric coupler design with different tap line ($y$) and bus line ($x$) core sizes.

(i) The proposed device includes a linear taper at the end of the tap line which allows the tap line with the smaller width to be coupled to a step index 1 mm POF fiber.

(ii) The proposed device uses a hollow waveguide structure whereas the asymmetric Y-junction is based on a two different materials (for the core and cladding).

(iii) The proposed device only requires one direction of operation.

The TOFR or the ratio of the power exiting the tap line ($y$) to the sum of power incident ($x$) and tap line is given by Equation (2) below [8]:

$$TOFR = \frac{y}{y + x} \tag{2}$$

However, this relationship applies to a solid core guide only. In a hollow structure, a higher loss is expected due to the dependency of the attenuation coefficient on $1/r^3$ and $1/R$ where $r$ and $R$ are the core radius and bending radius of the waveguide respectively [9]. In addition, we expect further losses to occur for the actual device which is due to the attenuation induced by the separation of the input and output fibers [10]. This attenuation, $\alpha$ as shown in the relationship below is dependent on the separation between the input and output fibers [10]. However, due to restriction on the ray tracing tool and ease of modeling, we have not included the attenuation due to this factor.

$$\alpha = -10 \log (1 - 2sA_N/3nd) \tag{3}$$

where $s$ is the fiber separation, $A_N$ is the numerical aperture of the fibers, $n$ is the refractive index and $d$ is the fibers core diameter.

The basic structure for the optical code generating device will be the $1 \times 2$ asymmetric coupler. We have set one branch to be the main bus line with a core size of 1 mm and another branch will be the tap line. Fig. 3 shows example of the $1 \times 2$ asymmetric coupler design with different tap line width. In this example, three different tap line widths have been utilized, 50%, 41% and 33% TOFR. These correspond to the tap width ($y$) of 1 mm, 0.7 mm and 0.5 mm, respectively.

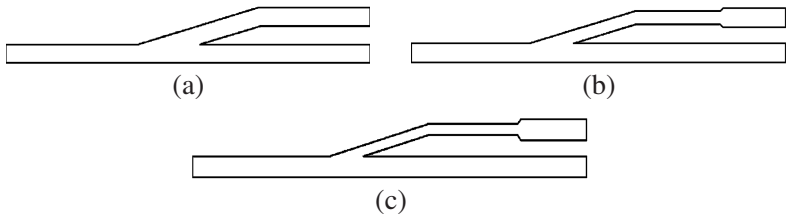


**Figure 3.** $1 \times 2$ asymmetric coupler with, (a) 50% TOFR, (b) 41% TOFR, and (c) 33% TOFR.

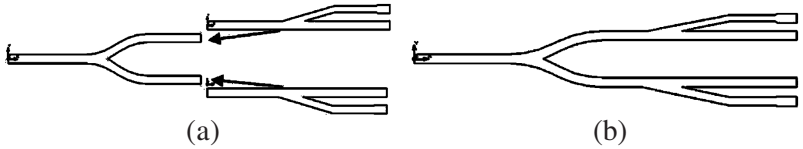


**Figure 4.** $1 \times 4$ coupler construction, (a) $1 \times 2$ Y-branch coupler before joining with two $1 \times 2$ asymmetric couplers, (b) $1 \times 4$ coupler with asymmetric branches.

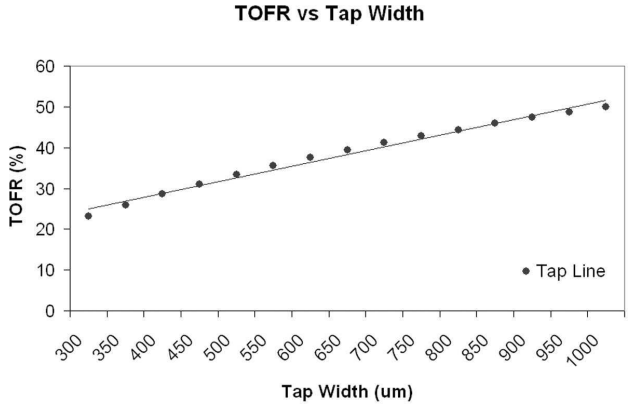


**Figure 5.** Design TOFR vs Tap Width for a $1 \times 2$ asymmetric coupler.

Higher order or $1 \times N$ asymmetric coupler can be constructed easily by cascading a $1 \times 2$ Y-branch coupler with two or more $1 \times 2$ asymmetric couplers. For example, in a $1 \times 4$ asymmetric coupler design, a $1 \times 2$ Y-branch coupler is cascaded with two $1 \times 2$ asymmetric couplers. The Y-branch coupler will provide a 50% power splitting at the output port. In order to complete the $1 \times 4$ coupler structure, two asymmetric $1 \times 2$ couplers are inserted. The concept of cascading the designs is shown in in Fig. 4.

The design results for the TOFR against the tap width for the $1 \times 2$ asymmetric coupler is given in Fig. 5. This results are obtained by taking on the ratio of the tap line to the sum of the tap line and bus line as in Equation (2), from $y = 300\,\mu m$ until $y = 1000\,\mu m$ with a bus line width of $1000\,\mu m$. The TOFR obtained using this range of tap line widths are from 23% to 50%. These results show that there is a linear relationship between the TOFR and the tap width.

## 3. DEVICE MODELING

The modeling and simulation of the $1 \times 2$ asymmetric coupler is done using non-sequential ray tracing. As we are interested in the TOFR characteristics of the asymmetric coupler design, we have adopted a hollow waveguide structure for modeling the waveguide properties. The hollow waveguide structure allows a more flexibility in guiding light rays without the restriction of the material's refractive index. By having this structure, we can model the asymmetric coupler's TOFR without the constraint of the attenuation due to absorption and scattering effects.

In the model structure, the inner-surface of the hollow waveguide region is defined as reflective where the material coating is written as metal coating. The wavelength used in this simulation is 650 nm, with input power of 1.0 mW. The hollow coupler is constructed by building a rectangular block, inserting the 3D coupler structure into it and then subtracting this object from the main rectangular block, shown in Figs. 6 and 7 for the $1 \times 2$ and $1 \times 4$ asymmetric couplers respectively.

The ray tracing diagram of several $1 \times 2$ asymmetric POF couplers is shown in Fig. 8. The ray tracing diagram shows the $1 \times 2$ asymmetric POF couplers with TOFR of 50%, 41% and 33% for tap line widths of $1000\,\mu m$, $700\,\mu m$ and $500\,\mu m$, respectively.

In the device design, the split angle, $\theta$ was initially set at 11°. Optimization of the TOFR has been performed by reducing the angle

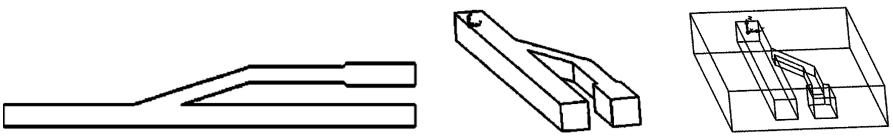


**Figure 6.** $1 \times 2$ asymmetric hollow coupler, (a) 2D layout, (b) 3D layout, (c) 3D hollow structure.

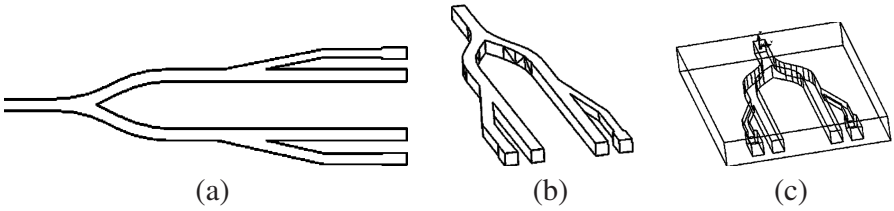


**Figure 7.** $1 \times 4$ asymmetric hollow coupler, (a) 2D layout, (b) 3D layout, (c) 3D hollow structure.

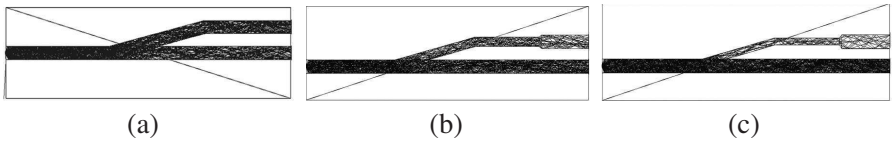


**Figure 8.** Ray tracing of $1 \times 2$ asymmetric coupler, (a) 50% TOFR, (b) 41% TOFR, (c) 33% TOFR.

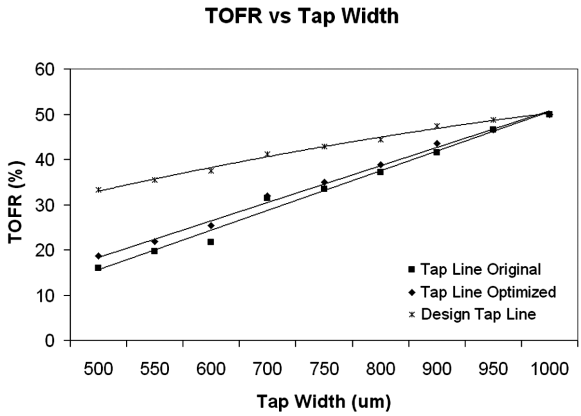


**Figure 9.** TOFR vs Tap Width: design and simulation (before and after optimization).

between the tap line and bus line. The angle is reduced from 11° to 6° where 6° is chosen to allow a minimum output ports spacing of 150 μm for a design TOFR value of 23%. This angle is fixed throughout the design process which allow us to control only the tap line width. The device length is reduced from 30 mm to 20 mm.

Figure 9 shows the TOFR vs Tap Width for the design, simulation before and simulation after optimization. All three plots of the TOFR show a linear relationship between the tap width and the TOFR. The

large variation of the TOFR is observed for the smaller TOFR which is due to the increase of attenuation as the core size of the tap line decreases. As the tap line width reduces, the higher order modes will be suppressed and not able to propagate into the smaller waveguide region (tap line). The TOFR obtained for the $1 \times 2$ asymmetric coupler based on the optimized design is from 18.6% and up to 49.9%. The results show the TOFR has improved 100% for the larger TOFR whereas the smaller TOFR, improved by only 17%.

The modeling and ray tracing of a $1 \times 4$ asymmetric coupler is done by first partitioning the device, which is shown in Fig. 10. The device structure is partitioned into six sections as shown in the figure. A simple 50% split is achieved using a Y-branch splitter (Sections A and B). If the input power is label $P_0$, then A and B will have output power of $0.5P_0$. Once the optical power is split by 50% at these two sections, the asymmetric coupler design in Sections C, D, E and F will split the $0.5P_0$ into smaller fractions of optical power, based on the actual design of the $1 \times 2$ asymmetric coupler. In this example, Sections C and D are part of the $1 \times 2$ asymmetric coupler design using 50 : 50 ratio design with the tap core width (C) of 1000 µm. In addition, Sections E and F are part of the $1 \times 2$ asymmetric coupler design using 32 : 65 ratio design (32 and 65 are values obtained from the ray tracing results of this $1 \times 2$ coupler). The tap core width (E) is 700 µm. For an example, at Section C, the output power detected (as a fraction of the input power) will be:

$$P_{out}(C) = \frac{50}{100} \times P_0 = 0.25P_0 \tag{4}$$

Table 1 shows the five designs of the $1 \times 4$ asymmetric coupler showing the branches C, D, E and F with their respective tap line and bus line widths.

**Table 1.** $1 \times 4$ asymmetric coupler designs: output branch width sizes.

| Design No. | Branch C–D | | Branch E–F | |
|---|---|---|---|---|
| | C Tap Width (µm) | D Bus Line (µm) | E Tap Width (µm) | F Bus Line (µm) |
| 1 | 900 | 1000 | 700 | 1000 |
| 2 | 500 | 1000 | 500 | 1000 |
| 3 | 1000 | 1000 | 700 | 1000 |
| 4 | 600 | 1000 | 800 | 1000 |
| 5 | 1000 | 1000 | 500 | 1000 |

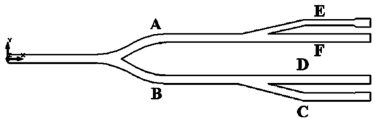


**Figure 10.** Partitioning the $1 \times 4$ POF waveguide coupler.

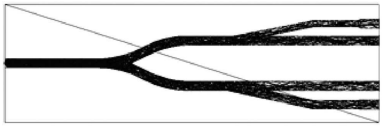

**Figure 11.** Ray tracing of a $1 \times 4$ asymmetric coupler.

**Table 2.** Output power for $1 \times 4$ asymmetric coupler.

| Design No. | Design | | | | Simulation | | | |
|---|---|---|---|---|---|---|---|---|
| | C | D | E | F | C | D | E | F |
| 1 | 0.20 | 0.28 | 0.15 | 0.32 | 0.22 | 0.27 | 0.15 | 0.32 |
| 2 | 0.08 | 0.38 | 0.08 | 0.38 | 0.08 | 0.39 | 0.08 | 0.39 |
| 3 | 0.25 | 0.25 | 0.15 | 0.32 | 0.30 | 0.20 | 0.15 | 0.32 |
| 4 | 0.11 | 0.37 | 0.18 | 0.31 | 0.12 | 0.39 | 0.17 | 0.28 |
| 5 | 0.25 | 0.25 | 0.08 | 0.38 | 0.26 | 0.22 | 0.08 | 0.40 |

The ray tracing result for a $1 \times 4$ asymmetric coupler is illustrated in Fig. 11. The design and the simulation results for five sets of $1 \times 4$ asymmetric couplers are shown in Table 2. The design values are based on the simple arithmetic shown in Equation (4) whereas, the simulation values are those obtained from the simulation. These values are the output power relative to the input power, $P_0$.

Table 2 shows the output power for the $1 \times 4$ asymmetric couplers, demonstrating the design and simulation effective power values at the output ports (C, D, E and F). The results shown in Table 2 demonstrated that the each of the $1 \times 2$ asymmetric coupler splits the incoming power from the Y-branch splitter appropriately based on the TOFR-Tap width design rule. As per design, each of the simulated output port corresponds close to the required design value.

## 4. FABRICATION AND CHARACTERIZATION

The mold insert for the device is prepared by engraving the device structure using high speed desktop CNC machine. We have previously reported the design and fabrication of a $1 \times 2$ Y-branch POF coupler based on a metal-based hollow taper waveguide structure with an insertion loss of about 8.2 dB and an excess loss of about 5 dB. The coupling ratio is almost 50 : 50 [11].

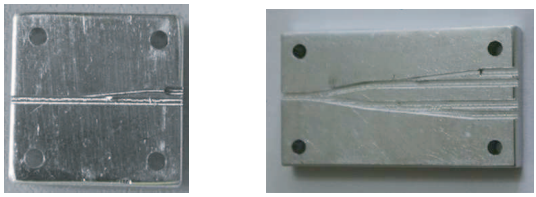

(a) (b)

**Figure 12.** Mold insert for (a) $1 \times 2$, (b) $1 \times 4$ asymmetric coupler devices.

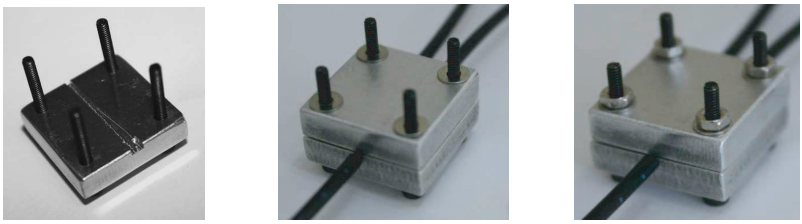

(a) (b) (c)

**Figure 13.** Assembling of the $1 \times 2$ asymmetric coupler, (a) mold insert with connecting screws, (b) fibers insertion and top plate placement, (c) connecting screws are secured.

One of the key advantage of this developed POF couplers is the simplification of the fabrication steps. In this process, a rigid mold insert is designed and fabricated using a CNC machining tool. This technique is a maskless process which significantly reduced the highly cost of producing photomask, and the costly photolithographic equipment. In this project, we used Roland's EGX-400 desktop CNC engraver to engrave the design structure drawn in CAD tool onto the metallic block. The endmill tool size used is 0.5 mm and machine spindle speed of 30,000 rpm has been utilized. In addition to the engraved device structure, 4 holes are drilled at each corner to allow a top metal plate to be screwed on top and enclosed the device structure. Fig. 12(a) is the mold insert for the $1 \times 2$ asymmetric device whereas Fig. 12(b) is the mold insert for the $1 \times 4$ asymmetric device.

After the mold insert has been fabricated, a top metal plate is positioned and the connecting screws are secured. Finally, short POF fibers (20 cm) are inserted into the input and output ports until the fibers are positioned just about 1 mm into the engraved slots. Fig. 13(a) shows the assembled device before the POF fibers are inserted whereas Fig. 13(b) shows the POF fibers after insertion into the device. Fig. 13(c) shows the assembled device structure with the

input and output POF fibers. Similarly, Figs. 14(a) and (b) show the assembling of the $1 \times 4$ asymmetric coupler devices.

The asymmetric POF couplers have been tested for its insertion loss. The insertion loss of this device has been tested using Advanced Fiber Solution FF-OS417 optical source at 650 nm and optical power meter OM210. The effective input power is 0 dBm. The insertion loss for the $1 \times 2$ asymmetric coupler at the tap line varies from 9 dB to 16 dB whereas for the bus line, the insertion loss is about $9 \pm 0.8$ dB. The insertion loss for the $11 \times 4$ asymmetric coupler at the output ports varies from 14 dB to 22 dB.

Figure 15 is the plot of the TOFR vs Tap Width for the metal-based fabricated devices. In addition, coupling ratios for the bus line are also included in both plots. In this plot, the TOFR varies from as small as 10.7% and up to 47.7% by a simple variation of the tap line width.

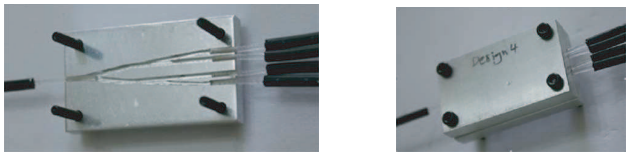

(a) (b)

**Figure 14.** Assembling of the $1 \times 4$ asymmetric coupler, (a) mold insert with connecting screws and fibers insertion, (b) top plate placement and connecting screws are secured.

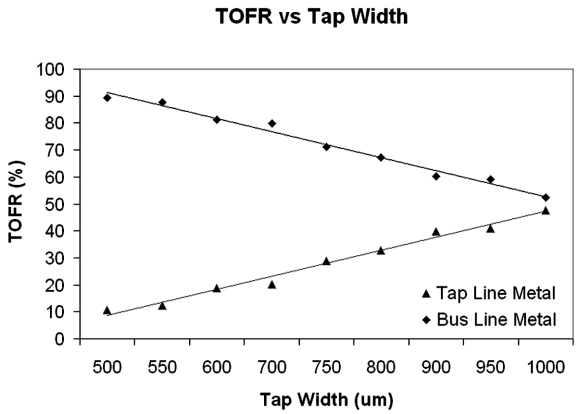


**Figure 15.** TOFR vs Tap Width for the fabricated $1 \times 2$ metal-based asymmetric coupler.

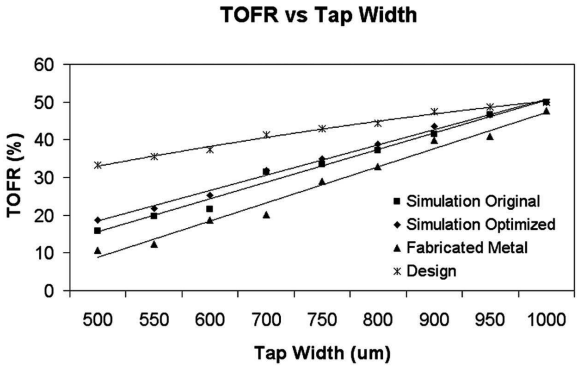


**Figure 16.** TOFR vs Tap Width for $1 \times 2$ asymmetric coupler (Design, Simulation and Fabricated Devices).

Figure 16 shows the plot of the TOFR against Tap Width for the design, simulated (original and optimized) and fabricated devices. The simulated optimized design structure and the fabricated metal-based devices shows TOFR variations from 18.6% to 49.9% and 10.7% to 47.7% respectively. A large variation on the lower TOFR of about 8% can be seen between this optimized device and the fabricated devices. In the fabricated device structure, the fact that the input and output POF fibers are separated by a distance in a hollow confinement, then there will be an induced attenuation due to the fiber separation. The longer the separation of the fibers, the higher the attenuation will be. The attenuation caused by the separation of two fibers is given by Equation (3) [10]. Apart from the large attenuation due to the separation between the input and output fibers, the large variation of the TOFR is mainly due to the structure imperfection of the fabricated device. This will cause the available optical power at the tap line to reduce significantly compare to the desired design value. As for the larger TOFR, the variation is less significant as the tap line widths are much bigger and hence allow higher order modes to enter the tap line.

The portable access-card system is designed where it can detect even the smallest output power. The system only uses short distance of POF fibers. In the prototype system, 650 nm LED light sources, which have optical power of 200 µW to 325 µW are utilized. The photodetectors used can detect optical power at the microwatt level and has a sensitivity down to $-55$ dBm (0.3 µW). Hence, in theory, for the minimum 1% of input power, then the following will hold. Assuming we use the 200 µW and the 325 µW light sources, and our detector has a sensitivity down to $-55$ dBm. The higher order devices, i.e., $N = 4$, 8 and 16 are constructed using the cascading technique

shown in Fig. 4 where 1 or more $1 \times 2$ Y-branch coupler is used (with 3 dB insertion loss). For instance, if $N = 4$, then only one Y-branch coupler; $N = 8$, two Y-branch couplers; and $N = 16$, three Y-branch couplers. Table 3 shows the power budget for the $1 \times N$ asymmetric POF coupler.

The $1 \times 4$ asymmetric coupler results for both simulated and fabricated devices are given in Table 4 and Table 5. For comparison, we have obtained the ratio of the output power for each of $1 \times 2$ asymmetric coupler component. For example, the output power ratios for the simulated and fabricated devices should be consistent even though, the effective value for the power will differ from each other. This is shown in the columns D/C and F/E.

In Table 5, if we consider the actual fabricated devices, the minimum detected power is about 0.0017 mW or 1.7 µW. This is still within the detectable value for the output power for a detector sensitivity of −55 dBm. Hence, for an actual fabricated device, the TOFR of a $1 \times 4$ POF coupler can go down to the design TOFR of 33% (tap width of 0.5 mm) or about 10.7% for the actual TOFR of the $1 \times 2$ asymmetric coupler.

**Table 3.** Power budget for $1 \times N$ asymmetric POF coupler.

| *Input Power* (µW) | *N* | *Min. Output Power* (µW) @ 1% |
|---|---|---|
| 200 | 2 | 2 |
| 200 | 4 | 1 |
| 200 | 8 | 0.5 |
| 325 | 16 | 0.4 |

**Table 4.** Output power ratios for $1 \times 4$ asymmetric coupler: simulated devices.

| Design No. | Simulated | | | | Branch Ratios | |
|---|---|---|---|---|---|---|
| | C | D | E | F | D/C | F/E |
| 1 | 0.22 | 0.27 | 0.15 | 0.32 | 1.22 | 2.13 |
| 2 | 0.08 | 0.39 | 0.08 | 0.39 | 4.87 | 4.87 |
| 3 | 0.30 | 0.20 | 0.15 | 0.32 | 0.66 | 2.13 |
| 4 | 0.12 | 0.39 | 0.17 | 0.28 | 3.25 | 1.64 |
| 5 | 0.26 | 0.22 | 0.08 | 0.40 | 0.84 | 5.00 |

**Table 5.** Output power ratios for $1 \times 4$ asymmetric coupler: fabricated devices.

| Design No. | Fabricated * | | | | Branch Ratios | |
|---|---|---|---|---|---|---|
| | C | D | E | F | D/C | F/E |
| 1 | 0.0045 | 0.0056 | 0.0083 | 0.0186 | 1.25 | 2.24 |
| 2 | 0.0017 | 0.0079 | 0.0026 | 0.0123 | 4.64 | 4.73 |
| 3 | 0.0089 | 0.0067 | 0.0069 | 0.0134 | 0.75 | 1.94 |
| 4 | 0.0022 | 0.0058 | 0.0079 | 0.0107 | 2.64 | 1.35 |
| 5 | 0.0123 | 0.0072 | 0.0034 | 0.0147 | 0.58 | 4.32 |

* the number in the columns C, D, E and F are multiply by $10^{-3}$.

## 5. CONCLUSION

A novel optical code generating device for a newly developed portable optical access-card system, based on $1 \times 2$ and $1 \times 4$ asymmetric POF couplers have been designed and fabricated. The asymmetric couplers have been constructed using hollow waveguide structure where the devices have been fabricated and assembled using metal-based mold inserts, produced using CNC machining technique. The $1 \times 2$ assembled devices show a simple linear characteristics of the TOFR against the tap width which corresponds to that of the designed and simulated device. The design devices shows a TOFR variation from 33% up to 50%, while the simulated devices shows a TOFR variation from 18.6% to 49.9% whereas the TOFR for the fabricated metal-based devices varies from 10.7% up to 47.7%, for a tap width of 500 µm to 1 mm. The fabricated $1 \times 4$ asymmetric coupler devices have shown similarity to that of the modeled devices. High excess loss of the fabricated devices is expected due to the attenuation introduce by the separation of the input and output fibers in the hollow structure design. Even with this high excess loss, the system is designed where it can detect even the smallest output power. In the fabricated $1 \times 4$ POF couplers, the minimum detected power is about 0.0017 mW or 1.7 µW which is still within the detectable value for the output power for a detector sensitivity of $-55$ dBm.

## ACKNOWLEDGMENT

The authors would like to thank Universiti Teknologi MARA and Universiti Kebangsaan Malaysia for the technical and financial support on this project.

## REFERENCES


1. Zubia, J. and J. Arrue, "Plastic optical fibers: An introduction to their technological processes and applications," *Optical Fiber Technology*, Vol. 7, 101–140, 2001.
2. Kalymious, D., "Plastic Optical Fibres (POF) in sensing — Current status and prospects," *17th International Conference on Optical Fibre Sensors, Proc. SPIE*, Vol. 5855, 1–4, 2005.
3. Buckley, N. I., "Codeable card and card-reading apparatus thereof," UK Patent 2022300, May 10, 1979.
4. Borough, H. C. and D. A. Pontarelli, "Encoded card employing fiber optic elements," US Patent 3728521, April 17, 1973.
5. Gary, C. K. and M. Ozan, "Security system responsive to optical fiber having Bragg gratings," US Patent 5633975, May 27, 1997.
6. Defense and Nuclear Technologies and Engineering Directorate, "Putting thieves on notice," *Science and Technology Review*, 4–5, Lawrence Livermore National Laboratory, October 1998.
7. Ehsan, A. A., S. Shaari, M. K. Abd Rahman, and K. M. R. Kee Zainal Abidin, "Hollow optical waveguide coupler for portable access card system application," *Journal of Optical Communications*, Vol. 30, 67–73, 2009.
8. Henry, W. M. and J. D. Love, "Asymmetric multimode Y-junction splitters," *Journal of Optical and Quantum Electronics*, Vol. 29, No. 3, 379–392, 1997.
9. Nubling, R. K. and A. J. Harrington, "Launch conditions and mode coupling in hollow-glass waveguides," *Opt. Engineering*, Vol. 37, No. 9, 2454–2458, 1998.
10. Ziemann, O., J. Krauser, P. E. Zamzow, and W. Daum, *POF Handbook: Optical Short Range Transmission System*, Springer-Verlag, 2008.
11. Ehsan, A. A., S. Shaari, and M. K. Abd Rahman, "$1 \times 2$ Y-branch plastic optical fiber waveguide coupler for optical access-card system," *Progress In Electromagnetics Research*, PIER 91, 85–100, 2009.